Transient W-Band EPR Study of Sequential Electron Transfer in Photosynthetic Bacterial Reaction Centers

Jau Tang, Lisa M. Utschig, Oleg Poluektov, and Marion C. Thurnauer*

Chemistry Division, Argonne National Laboratory, Argonne, Illinois 60439

Received: January 20, 1999; In Final Form: April 19, 1999

Electron-spin polarized (ESP) EPR spectra at W-band (95 GHz) were obtained for deuterated Fe-removed/Zn-substituted photosynthetic bacterial reaction centers (RCs) to investigate the influence of the rate of charge separation on the observed $P^+Q_A^-$ charge separated state. Temperature dependent ESP EPR spectra for kinetically characterized Zn-substituted RCs from *Rb. sphaeroides* R-26 having different rates (k_Q) of the electron transfer from the bacteriopheophytin to the quinone acceptor were obtained. The Zn−RCs exhibited either the native "fast" $(200\ ps)^{-1}$ k_Q or a "slow" $(3-6\ ns)^{-1}$ k_Q at 298 K as determined from transient optical measurements. Sequential electron-transfer polarization modeling of the polarized W-band EPR spectra obtained with these samples was used to address the reason for the differences in the electron-transfer rates. Herein, we report the k_Q rate constant, the temperature dependence of k_Q, and the reorganization energy for the $P^+H^-Q_A$ and $P^+HQ_A^-$ electron-transfer step determined from SETP modeling of the experimental spectra. The reorganization energy for the electron-transfer process between $P^+H^-Q_A$ and $P^+HQ_A^-$, and not structural changes in the donor or acceptor, was found to be the dominant factor that is altered during Fe-removal procedures.

Introduction

The key reaction of photosynthetic solar energy conversion involves the photoexcitation of a primary donor (P) followed by rapid, sequential electron transfer to a series of acceptors resulting in charge separation. In the purple bacterial reaction center (RC) protein, the primary radical pair P^+H^-, where H denotes a monomeric bacteriopheophytin, is formed within ∼3 ps of photoexcitation of the special pair of bacteriochlorophylls (P). Within about 200 ps at 295 K the electron is transferred from H^- to the primary ubiquinone acceptor (Q_A) yielding the membrane-spanning secondary radical pair $P^+Q_A^-$. Within 200 μs, the electron reaches the final quinone acceptor Q_B. Transient EPR spectroscopy has been extensively used in the study of the radical pair $P^+Q_A^-$. (For reviews, see ref 1−3.) The spin-polarized spectrum of this state provides structural information about the spin system, such as the distance between and relative orientation of donor and acceptor cofactors. Also, insight into the interaction of the radicals with the protein environment as well as kinetic information about the sequential charge separation process can be obtained. The use of high field W-band (95 GHz) EPR results in highly resolved spectra, providing enhanced structural information. (See, for example, refs 4−7.) Recent computer simulations at W-band have demonstrated the potential application of high field EPR in probing fast sequential electron-transfer processes that occur within a few hundred picoseconds.[8,9] Ultimately, high-field transient EPR can be used to elucidate the importance of donor/acceptor geometry versus protein reorganization energy in regulating photosynthetic electron-transfer processes.

Metal ion and protein subunit manipulation of the RC provide control over the electron-transfer rate (k_Q) from the H to Q_A.

* Corresponding author. Chemistry Division D-200, Argonne National Laboratory, 9700 S. Cass Ave., Argonne, IL 60439. Phone: (630) 252-3570. Fax: (630) 252−9289. E-mail: thurnauer@anlchm.chm.anl.gov.

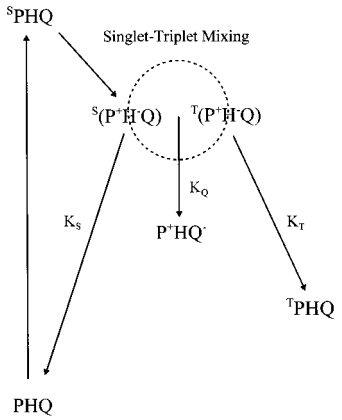

Figure 1. Simplified scheme of the radical pair states and the electron transfer and decay pathways in bacterial RCs. ^{T}P is the molecular triplet state of the primary donor, H the bacteriopheophytin, and Q is the primary quinone acceptor Q_A.

Optical measurements by Kirmaier et al. indicated a reduction of the electron-transfer rate k_Q in iron-depleted RCs from *Rhodobacter sphaeroides* R26.[10] The lifetime of P^+H^- increased to approximately 4 ns as compared to the 200 ps lifetime observed in native Fe-containing RCs. Because of the long-lived P^+H^- state, two decay pathways, charge recombination to the ground state (k_S) and triplet formation (k_T), compete with the electron transfer to Q_A (k_Q), complicating the direct determination of k_Q (Figure 1). The P^+H^- lifetime has been shown to be preparation dependent, varying between the native 200 ps and the "slow" 4 ns with Fe-removal and/or Zn-substitution with or without the H-subunit removed.[10−13] Recently, we have redefined the Fe-removal procedures and found that the observed long-lived P^+H^- state in Fe-removed RCs is H-subunit-independent, and in some cases, independent of Fe-site occupancy as Zn substitution does not ensure retention

10.1021/jp990236t CCC: $18.00
Published on Web 06/02/1999

of the native k_Q.[14] Many interesting questions remain concerning the observed changes in P^+H^- lifetime. What is the value of k_Q at low temperature? What is the reason for the change in electron-transfer rates of k_Q? There are several possible explanations for the dramatic change in P^+H^- lifetime that may involve either structural changes in the orientation of the cofactors or protein reorganization energy.[10,12]

Analysis of highly resolved electron spin polarized (ESP) EPR spectra of samples with native versus "slow" k_Q could potentially elucidate the dominant factors that regulate this electron-transfer process. ESP signals are sensitive to the geometry of the observed radical pair ($P^+Q_A^-$) and can provide structural information about the intermediate radical pair (P^+H^-). The correlated radical pair polarization (CRPP) model[15−17] has been used to interpret the observed polarized EPR spectra for the RC proteins of photosystem I (PSI) and purple bacteria.[4,7,18] In these studies, the lifetime of radical pairs preceding the observed radical pairs is assumed to be very short and the observed radical pairs are practically in a pure singlet state initially. However, if the lifetime is not sufficiently short or the singlet−triplet mixing becomes extremely fast due to strong Zeeman interactions at high magnetic fields, one has to consider the sequential electron-transfer polarization (SETP) model by including both the observed and the preceding radical pairs.[8,9,19−22] Although the intermediate radical pairs may not be directly detectable, having a lifetime of a few hundred picoseconds can cause sufficient singlet−triplet mixing at high fields. Significant spectral changes in the polarized W-band spectra were demonstrated by simulation even if the lifetime is only a few hundred picoseconds.[8]

The experimental X- (9 GHz) and Q-band (34 GHz) transient EPR spectra of the radical pair state $P^+Q_A^-$ of kinetically characterized deuterated Fe-removed RCs with native or "slow" k_Q showed significant differences in zero crossing points and relative amplitudes of polarization.[14] These differences reflected the trends in polarization predicted from the SETP model, although the results indicated that k_Q at liquid helium temperature may be 1 ns^{-1}.[14] Herein, we extend our previous work by reporting highly resolved W-band spectra of deuterated Fe-removed RCs with native or "slow" k_Q. These spectra represent the first high field experimental data which display SETP. On the basis of the SETP model, we can measure the rate constant k_Q and its temperature dependence for the electron transfer between $P^+H^-Q_A$ and $P^+HQ_A^-$. The results implicate an important role for protein reorganization energies in regulating electron-transfer processes.

Materials and Methods

RC Samples. Deuterated reaction centers were isolated from whole cells of *Rb. sphaeroides* R-26[14] which were grown in D_2O (99.7%) on deuterated substrates.[23] The RCs were isolated, and the Fe removed with Zn-substitution into the Fe site as previously described.[14] The metal content characterization and room-temperature transient absorption measurements of the 670 nm bacteriopheophytin anion band for these specific RC samples are detailed in our previous paper.[14] Herein, we describe the high field EPR spectra obtained on the identical two deuterated Zn−RC samples from which we reported the transient EPR spectra at X- and Q-band, one that exhibits the "fast" (200 ps)$^{-1}$ k_Q and the second that exhibits the "slow" k_Q of (3−6 ns)$^{-1}$.

EPR Measurements. The electron spin−echo measurements were performed using a home-built W-band (94.9 GHz) spectrometer in the laboratory of J. Schmidt at Leiden.[24] The RC samples were placed in a quartz tube and then mounted in a cylindrical cavity. Samples were shock frozen to 77 K in the dark within the cavity and then gradually cooled to liquid helium temperature. The temperature was regulated by flowing liquid helium through the cryostat. A two-pulse echo sequence was used to obtain the data. Typically, the time interval between pulses was 200−300 ns, with pulse widths of 50−90 ns. The repetition rate of the pulse sequence was 1−5 Hz. To create the photoinduced polarized spectra, an optical parametric oscillator (GWU, OPO-C355) pumped by a frequency doubled Nd:YAG laser (Continuum, Surelite I) was used. A laser pulse of 10 ns was positioned 500 ns before the first microwave pulse. The spin-polarized spectra were recorded by monitoring the integral intensity of the echo using a boxcar integrator as a function of the magnetic field. The spectra were obtained for each sample at temperatures ranging from 40 to 150 K.

The SETP Model. To model sequential electron transfer in bacterial photosynthesis, we consider charge separation processes that take place by electron transfer from the photoexcited state of D_1 to $D_1^+A_2^-A_3$ and then to $D_1^+A_2A_3^-$. As illustrated in Figure 1, the donor D_1 is the primary donor P, A_2 the intermediate acceptor H, and A_3 the primary quinone Q_A. Evolution of the density matrix involves two stages. The details of the SETP model have been presented in our earlier work.[8,20] For the clarity of the presentation, only the key and relevant equations are reiterated here. The evolution for the density matrix ρ_{12} for the initial radical pair $D_1^+A_2^-$ is given by

$$\rho_{12}(t) = e^{-\frac{i}{\hbar}H_{12}t}\,\rho_{12}(0)e^{\frac{i}{\hbar}H_{12}^{+}t}$$

$$H_{12} = H_{12,0} - \frac{i}{2}\hbar\Gamma \tag{1}$$

$$\Gamma = k_T\left(\frac{3}{4} + S_1\cdot S_2\right) + k_S\left(\frac{1}{4} - S_1\cdot S_2\right) + k_Q$$

$H_{12,0}$ describes the magnetic interactions as

$$H_{12,0} = \beta B_0(g_{1,\mathrm{eff}}S_{1z} + g_{2,\mathrm{eff}}S_{2z}) + S_{1z}\sum_\alpha A_{1\alpha}I_{\alpha z} + S_{2z}\sum_\alpha A_{2\alpha}I_\alpha$$

$$+ \frac{d_{12}}{2}(3\cos^2\theta_{D,12} - 1)\Big[(S_{1z} + S_{2z})^2 - \frac{1}{3}(S_1 + S_2)\cdot(S_1 + S_2)\Big] \tag{2}$$

$$- J_{12}\left(\frac{1}{2} + 2S_1\cdot S_2\right)$$

and the non-Hermitian part $-i\hbar\Gamma/2$ describes the decay processes with k_S and k_T, the decay rate constants for the singlet and the triplet, and k_Q, the electron-transfer rate constant from $D_1^+A_2^-$ to $D_1^+A_3^-$. The effective g-factor is defined as $g_{\mathrm{eff}} = (g_{xx}^2\sin^2\theta_{12}\cos^2\phi_{12} + g_{yy}^2\sin^2\theta_{12}\sin^2\phi_{12} + g_{zz}^2\cos^2\theta_{12})^{1/2}$. Assuming a singlet precursor, the evolution of $\boldsymbol{\rho}_{13}(t)$ is given by

$$\rho_{13}(t) = k_Q\int_0^t d\tau\; e^{-\frac{i}{\hbar}H_{13}(t-\tau)}e^{-\frac{i}{\hbar}H_{12}\tau}\rho_{12}(0)e^{\frac{i}{\hbar}H_{12}^{+}\tau}e^{\frac{i}{\hbar}H_{13}(t-\tau)} \tag{3}$$

The polarized EPR spectrum for the radical pair $D_1^+A_3^-$ can be evaluated in the following. $\mathbf{H}_{13}$ can be diagonalized by a unitary matrix $\mathbf{U}_{13}$, and $\mathbf{U}_{13}\mathbf{H}_{13}\mathbf{U}_{13}^+$ is a diagonal matrix $\mathbf{\Lambda}_{13}$ with eigenenergies $\lambda_{13,1}$ and $\lambda_{13,2}$ as given by $-d_{13}(\cos^2\theta_{D,13} - 1/3)/2 \mp \omega_{13}/2$ and $\omega_{13} = (P_{13}^2 + Q_{13}^2)^{1/2}$, where $P_{13} = 2J_{13} +$

$d_{13}(\cos^2\theta_{D,13} - 1/3)$ and $Q_{13} = (g_{1,\text{eff}} - g_{3,\text{eff}})\beta B_0 + \Sigma(a_{1\alpha}m_{1\alpha} - a_{3\alpha}m_{3\alpha})$. $\mathbf{H}_{12}$ can be diagonalized by a nonunitary transformation $\mathbf{U}_{12}$ ($\mathbf{U}_{12}^{-1} \neq \mathbf{U}_{12}^{+}$). $\mathbf{\Lambda}_{12} = \mathbf{U}_{12}\mathbf{H}_{12}\mathbf{U}_{12}^{-1}$ is diagonal and the eigenenergies $\lambda_{12,1}$ and $\lambda_{12,2}$ are given by $-d_{12}(\cos^2\theta_{D,12} - 1/3)/2 - i\hbar(k_S + k_T + 2k_Q)/4 \mp \omega_{12}/2$ and $\omega_{12} = (P_{12}^2 + Q_{12}^2)^{1/2}$, where $P_{12} = 2J_{12} + d_{12}(\cos^2\theta_{D,12} - 1/3) + i\hbar(k_T - k_S)/2$ and $Q_{12} = (g_{1,\text{eff}} - g_{2,\text{eff}})\beta B0 + \Sigma(a_{1\alpha}m_{1\alpha} - a_{2\alpha}m_{2\alpha})$. The matrixes $\mathbf{U}_{12}$ and $\mathbf{U}_{13}$ are given by

$$\mathbf{U}_{12} = \begin{pmatrix} \cos\xi_{12} & -\sin\xi_{12} \\ \sin\xi_{12} & \cos\xi_{12} \end{pmatrix}, \quad \mathbf{U}_{13} = \begin{pmatrix} \cos\xi_{13} & -\sin\xi_{13} \\ \sin\xi_{13} & \cos\xi_{13} \end{pmatrix} \tag{4}$$

where $2\xi_{12} = -\tan^{-1}(Q_{12}/P_{12})$ and $2\xi_{13} = -\tan^{-1}(Q_{13}/P_{13})$. If $k_T \neq k_S$, P_{12} and ξ_{12} are complex numbers. ξ_{12} is the mixing angle between $|S\rangle$ and $|T_0\rangle$, and $|a\rangle = \cos\xi_{13}|S\rangle - \sin\xi_{13}|T_0\rangle$ and $|b\rangle = \sin\xi_{13}|S\rangle + \cos\xi_{13}|T_0\rangle$. The population can be calculated from eq 3 and

$$\langle a|\rho_{13}|a\rangle = k_Q[|\cos\xi|^2\sigma_{11} + |\sin\xi|^2\sigma_{22} - 2Re(\sigma_{12}\sin\xi^*\cos\xi)]$$

$$\langle b|\rho_{13}|b\rangle = k_Q[|\sin\xi|^2\sigma_{11} + |\cos\xi|^2\sigma_{22} - 2Re(\sigma_{12}\sin\xi\cos\xi^*)] \tag{5}$$

and

$$\sigma_{11} = i\hbar|\cos\xi_{12}|^2/(\lambda_{12,1}^* - \lambda_{12,1})$$

$$\sigma_{22} = i\hbar|\sin\xi_{12}|^2/(\lambda_{12,1}^* - \lambda_{12,2}) \tag{6}$$

$$\sigma_{12} = i\hbar\cos\xi_{12}\sin\xi_{12}^*/(\lambda_{12,1}^* - \lambda_{12,2})$$

where $\xi = \xi_{13} - \xi_{12}$.

The polarized EPR spectrum consists of two absorptive transitions between $|T_1\rangle$ and $|a\rangle$ with intensity $\langle a|\rho_{13}|a\rangle \sin^2\xi_{13}$ and between $|T_1\rangle$ and $|b\rangle$ with intensity $\langle b|\rho_{13}|b\rangle\cos^2\xi_{13}$. There are also two emissive transitions between $|T_{-1}\rangle$ and $|a\rangle$ with intensity $\langle a|\rho_{13}|a\rangle \sin^2\xi_{13}$, and between $|T_{-1}\rangle$ and $|b\rangle$ with intensity $\langle b|\rho_{13}|b\rangle\cos^2\xi_{13}$. The polarized EPR spectrum can be calculated from the transition frequencies and the corresponding intensity given in eqs 5 and 6. The eigenenergy for $D_1^+A_3^-$ is given by

$$E_{T_1} = -J_{13} + \frac{d_{13}}{2}\left(\cos^2\theta_{13} - \frac{1}{3}\right) + \frac{1}{2}(g_{1,\text{eff}} + g_{3,\text{eff}})\beta B_0 + \frac{1}{2}\left(\sum A_{1\alpha}m_{1\alpha} + \sum A_{3\alpha}m_{3\alpha}\right)$$

$$E_a = -\frac{\omega_{13}}{2} - \frac{d_{13}}{2}\left(\cos^2\theta_{13} - \frac{1}{3}\right)$$

$$E_b = -\frac{\omega_{13}}{2} - \frac{d_{13}}{2}\left(\cos^2\theta_{13} - \frac{1}{3}\right) \tag{7}$$

$$E_{T_{-1}} = -J_{13} + \frac{d_{13}}{2}\left(\cos^2\theta_{13} - \frac{1}{3}\right) - \frac{1}{2}(g_{1,\text{eff}} + g_{3,\text{eff}})\beta B_0 - \frac{1}{2}\left(\sum A_{1\alpha}m_{1\alpha} + \sum A_{3\alpha}m_{3\alpha}\right)$$

In the limit of large k_Q, these EPR transitions have equal intensity as in the CRPP model. An alternative approach adapted by Hore[22] using 4×4 matrices in Liouville space is equivalent to our earlier approach[20] that uses 2×2 matrices with a non-Hermitian Hamiltonian.

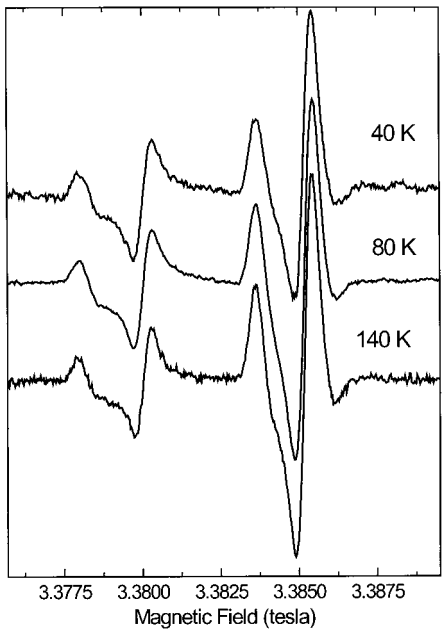

Figure 2. Temperature dependence of the spin-polarized W-band EPR spectra of deuterated Zn−RC sample with native k_Q. The spectra exhibit almost identical spin polarized patterns, indicating no temperature effect.

Results and Discussion

In this study, we examined the W-band ESP EPR spectra from two separate preparations of RCs where the rate of the electron transfer from the bacteriopheophytin to the quinone acceptor has been measured by transient optical absorption spectroscopy. Both samples were Fe-depleted and reconstituted with Zn^{2+}. One Zn−RC exhibited the native "fast" (200 ps)$^{-1}$ k_Q while the other exhibited a long-lived P^+H^- lifetime of (3−6 ns)$^{-1}$ at 298 K and thus a "slow" k_Q.[14] Thus far, the reason for these differences in k_Q remains unclear. Nonetheless, one possible explanation can be ruled out. It is unlikely that the observed differences in k_Q result from any metal-induced coulomb electrostatic fields at the site of the primary donor and acceptor since both samples have Zn^{2+} substituted into the Fe-site. Thus, the two main possibilities that remain involve specific changes in protein structure and/or reorganization energy that influence the $P^+H^-Q_A$ to $P^+HQ_A^-$ electron-transfer process. SETP modeling of the polarized W-band EPR spectra is used to address these possibilities.

The W-band transient EPR spectra of the kinetically defined deuterated Zn−RCs with fast k_Q are shown in Figure 2. The observed A/E/A/A/E/A polarization pattern and relative amplitude of each resonance within the spectra are nearly identical to previously published spectra.[7] Importantly, the ESP EPR spectra of the fast k_Q Zn−RC sample does not show any significant temperature dependence. In contrast, the ESP EPR spectrum of the slow k_Q Zn−RC sample, shown in Figure 3, is temperature dependent and exhibits noticeable spectral changes compared to the fast k_Q Zn−RC spectra. Figure 4 compares the ESP EPR spectra of the Zn−RCs with fast versus slow k_Q recorded at 80 K. The greatest variance is the high field region of the spectrum, with the high field emission being weaker and the high field absorption being stronger in the slow k_Q Zn−RC spectrum than in the fast k_Q Zn−RC spectrum. These spectral changes reflect the predicted trends expected from SETP modeling, i.e., for longer lifetimes of P^+H^-, the spectra reflect

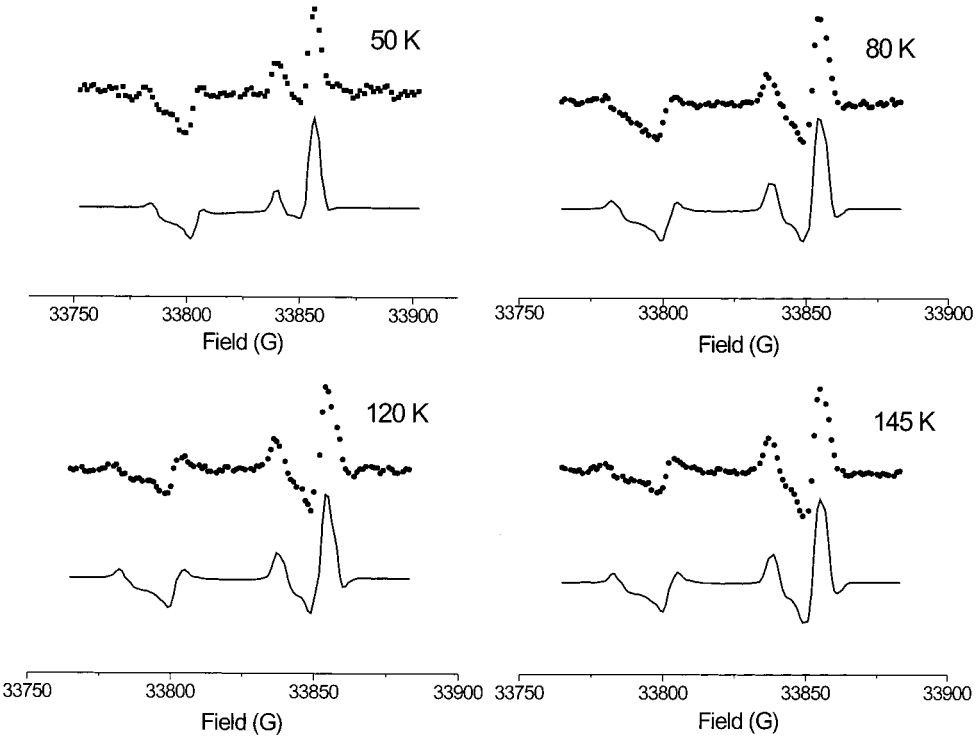

Figure 3. Spin-polarized W-band EPR spectra of the "slow" k_Q Zn−RC sample, showing noticeable spectral changes at four different temperatures. The dotted curves represent experimental data and the solid curves represent simulated data using the SETP model.

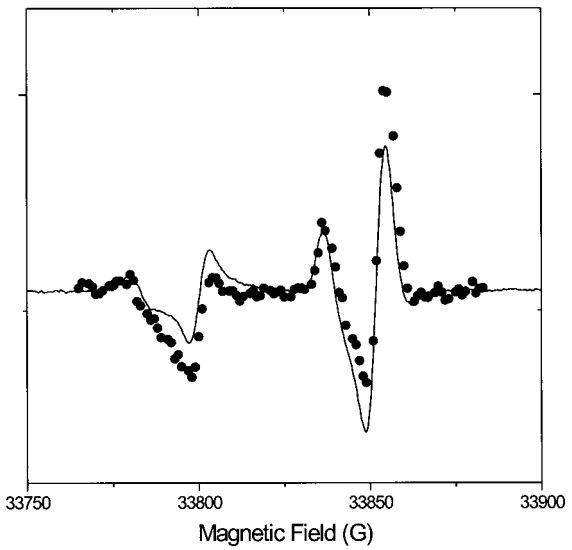

Figure 4. Comparison of the W-band $P^+Q_A^-$ ESP signals recorded at 80 K of Zn−RCs with "fast" and "slow" k_Q. The spin-polarized spectrum for Zn−RCs with $(200\ ps)^{-1}$ k_Q is shown in boldface and the corresponding spectrum for Zn−RC with 3−6 ns lifetime of P^+H^- (determined at 293 K) is dotted.

the transfer of chemically induced electron polarization (CIDEP)[20,21] from P^+H^-. To our knowledge, this is the first report of high field experimental data that exhibits SETP behavior.

The SETP model has been used to fit the temperature-dependent spectral data. These least-squares fits are depicted in Figure 3. In our analysis, we have assumed a specific structure for the radical pair $P^+Q_A^-$. There are three reported X-ray structures of the bacterial RC[25−27] and four indeterminate orientations (I−IV)[28] of the P^+ *g*-tensor. Substantial differences in the orientation angles exist for the dipolar tensor and the *g*-tensor for P^+ and Q_A^- among the three reported crystal

TABLE 1: Parameters for the Simulations in Figure 3

W-band: 33893 G
$1/k_S = 3.33 \times 10^2$ ns
$1/k_T = 2.5$ ns
$J_{12} = 7$ G, $d_{12} = -4.5$ G
$\Delta B_{1,pp} = 4.4$ G
$g_{1,xx} = 2.00333$, $g_{1,yy} = 2.00248$, $g_{1,zz} = 2.00209$
$\Delta B_{2,pp} = 4.6$ G
$g_{2,xx} = g_{2,yy} = g_{2,zz} = 2.0036$
$\theta_{D,12} = 55°$, $\phi_{D,12} = 57°$,
$J_{13} = 0$ G, $d_{13} = -1.24$ G
$\Delta B_{3,pp} = 3.7$ G
$g_{3,xx} = 2.00660$, $g_{3,yy} = 2.00548$, $g_{3,zz} = 2.00234$
$\phi_{13} = 23.0°$, $\theta_{13} = 119.3°$, $\psi_{13} = 18.3°$
$\theta_{D,13} = 71.6°$, $\phi_{D,13} = 68.5°$

structures.[29] For the reasons discussed extensively in an earlier paper,[30] we have used the geometry from the structure of Ermler et al.[26] with the *g* tensor orientation II (Ermler II) for our fits, but have let the *g*-value float in the fitting procedure. It is possible to obtain a reasonable fit with a different geometry, such as Ermler I or Komiya II, but slightly different *g*-values are necessary. The g_{xx}-component of Q_A^- was set to 2.00660 as a reference for microwave frequency calibration. The relevant geometric and magnetic parameters are listed in Table 1. The assumption of a specific geometry does not affect the conclusions from these experiments (see below). In addition, we have assumed that there is no temperature induced geometry changes of the radical pair $P^+Q_A^-$.

Significantly, preliminary results indicate that there is *not* a large structural change in the P^+ donor/Q_A^- acceptor geometry between "fast" and "slow" k_Q samples. Highly resolved X- and Q-band time-resolved radical pair quantum beats have been recorded for two separate preparations of Fe-depleted RCs with fast or slow k_Q rates. Expected qualitative differences in the spread of the phase angles are observed in the quantum beat EPR spectra for samples having different rates of k_Q. However, the quantum beats for both the fast and slow k_Q samples start out at zero amplitude and have the same frequency, indicating

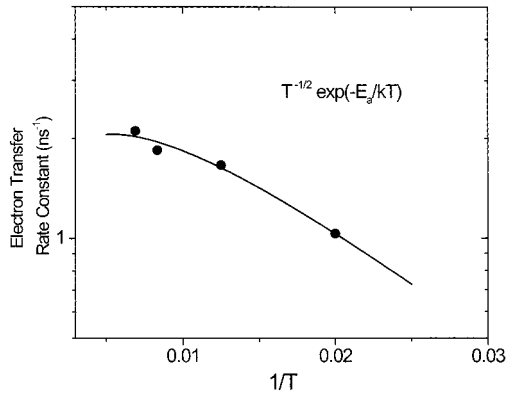

Figure 5. The temperature dependence of the k_Q electron-transfer rate as determined from the fitting of the polarized EPR spectra by the SETP model. The fit of the temperature dependence of k_Q gives an activation energy E_a of 65 cm^{-1}.

that both samples have the same geometry for $P^+Q_A^-$ (G. Kothe, unpublished results). In addition, measurement of out-of phase spin−echoes[31] for RCs with fast vs slow k_Q show that there is no significant difference in the distance between the donor P^+ and the acceptor Q_A^- (G. Kothe, unpublished results). Furthermore, low-temperature time-resolved EPR measurements show that the charge recombination electron-transfer rates from $P^+Q_A^-$ to the ground-state PQ_A are identical for RCs that exhibit different rates of k_Q. (O. Poluektov and L. M. Utschig, unpublished results.)

Using the SETP model we have ascertained the k_Q electron transfer rate at different temperatures directly from the transient EPR data. We have used a least-squares fitting procedure with the parameters in Table 1 to simulate the transient slow k_Q Zn−RC EPR spectra at four different temperatures in the range 50−150 K (Figure 3 and Table 1). We have found that, in this system of "slow" Zn−RCs, the electron-transfer rate exhibits the normal temperature trend of a decrease in rate coinciding with a decrease in temperature. The k_Q electron-transfer rate ranges from $\sim$ 1 ns^{-1} at 50 K to $\sim$ 500 ps^{-1} at 150 K. These results are confirmed by Q-band EPR studies that showed a relative increase in the ratio of light-induced triplet P signal to the P^+ signal as the temperature was lowered (data not shown). These results contrast with those of the native system. In native Fe-containing RCs, the k_Q electron-transfer rate has an unusual temperature dependence with an increase in rate as the temperature is lowered.[32] In the temperature range 300 to 100 K, the rate constant increases rapidly by a factor of approximately 2, and remains unchanged in the range of 100 to 4.2 K. Such a reversed temperature trend has been explained by Marcus theory with an activationless process. By fitting the temperature dependence exhibited by our slow k_Q Zn−RCs using the classical Marcus theory[33] (Figure 5), we have found a small activation energy of 65 cm^{-1}. Using this activation energy and a free energy gap of 5400 cm^{-1}, [34] we estimate the reorganization energy to be $\sim$ 6700 cm^{-1} for the slow k_Q sample. The $P^+H^-Q_A$ to $P^+HQ_A^-$ electron-transfer event, which was originally a quasi-activationless process in the native Fe-containing system, has an activation energy in the "slow" RCs. Thus, an increase in the reorganization energy by about 25% appears to be the main factor that alters the electron-transfer rate k_Q.

We have analyzed the significance of several parameters that influence the SETP spectral simulations: In our determination of k_Q by SETP modeling, we have assumed that the exchange interaction between P^+ and H^- is 7 G, as suggested by Budil et al.[35] If we had used the value of 5 G as suggested by Volk et al.,[36] the values of k_Q obtained from our fits would be reduced by about 20%. The overall temperature dependence, however, would remain basically unchanged and result in similar activation and reorganization energies. In the fitting of k_Q we have also assumed that k_T remains unchanged in the temperature range from 50 to 145 K. Even with a large change of $1/k_T$ from 2.5 to 1.5 ns, the simulated k_Q is found to change by less than 20%. Finally, the error of k_Q which is due to fitting experimental spectra with a given signal-to-noise ratio (while all other parameters are fixed) is estimated to be $\sim$20%. This means that the overall error for the absolute value of k_Q might be relatively large, mainly because of the lack of accurate data on the many parameters used in the simulation. But this error will not significantly influence the general temperature dependence of k_Q, discussed above.

Transient optical absorption measurements at room temperature of the decay of P^+H^- by ourselves and others[10,12,14] indicate a much slower electron-transfer rate than deduced herein (Figure 5), with a P^+H^- lifetime of approximately 4 ns. Because the overall decay rate of P^+H^- is the sum of k_Q, k_T and k_S, the largest possible value of k_Q is $(4\ ns)^{-1}$ which would occur in the absence of decays to the ground-state PHQ_A and triplet $^TPHQ_A$ (Figure 1). Thus, the k_Q deduced optically is much slower than the values determined from the fitting of the spin-polarized EPR spectra, presented in Figure 5. In this comparison between rates from optical (at 0 G) and EPR (at 33 KG) measurements, we have assumed that the rates k_T, k_S and k_Q are not very sensitive to changes in magnetic field (0 to 30 KG). A recent study has shown that recombination dynamics can be influenced by a field of several Tesla for a transition metal redox system having a large *g*-anisotropy.[37] We do not expect that these rates for RCs are significantly influenced by the magnetic field. This is justified by the experimental observation of little magnetic field effect on k_T reported by Chidsey et al.[38] Because in our fits k_Q is found to be the dominant process, the slight temperature dependence in k_T or k_S as reported by Chidsey et al. would not significantly change the fitted value of k_Q. In our simulation, a change of k_T by a factor of 2 causes less than 15% change in k_Q. Therefore, we believe that the activation energy determination by transient EPR techniques and the SETP modeling can be considered reliable.

Presently, we cannot explain the discrepancy in rates between the optical data and our EPR data.[39] Further measurements of the electron-transfer rates by transient optical techniques and their temperature dependence will help us understand why the rate of k_Q deduced from the optical measurements of the P^+H^- lifetime is slower than that determined from our fits to the transient EPR data. However, our data indicate that both structural changes in $P^+Q_A^-$ and metal induced Coulombic effects on $P^+Q_A^-$ do *not* induce the observed changes in k_Q electron-transfer rate. This result is consistent with other experiments that have shown large changes in the $P^+Q_A^-$ recombination or Q_A^- to Q_B electron-transfer rates can occur without large changes in the donor/acceptor geometries.[40−42] Thus, we conclude that activation energy for the electron-transfer process between $P^+H^-Q_A$ and $P^+HQ_A^-$ is the dominant factor that is altered in the "slow" Zn−RCs. This agrees with the observation of a normal temperature dependence. Assuming no change in the free energy of the reaction for the "fast" and "slow" samples, a 25% increase in the reorganization energy for the "slow" sample is determined. The observation of identical charge recombination electron-transfer rates from $P^+Q_A^-$ to the ground-state PQ_A for RCs that exhibit different rates of k_Q suggests that reorganization energy changes are not in the

vicinity of the primary donor or the quinone acceptor, but might occur around the bacteriopheophytin.

Acknowledgment. The authors express their appreciation to Prof. J. Schmidt for the use of his W-band EPR facilities. The essential contributions of G. Kothe and co-workers to this work are also acknowledged. We thank D. Tiede for helpful discussions. This work was supported by the U.S. Department of Energy, Office of Basic Energy Sciences, Division of Chemical Sciences, under Contract W-31-109-Eng-38.

References and Notes

(1) Angerhofer, A.; Bittl, R. *Photochem. Photobiol.* **1996**, *63*, 11.

(2) Molin, Y. N. *Spin Polarization and Magnetic Effects in Radical Reactions*; Elsevier: Amsterdam, 1984.

(3) Snyder, S. W.; Thurnauer, M. C. In *The Photosynthetic Reaction Center*; Deisenhofer, M., Norris, J., Eds.; Academic Press: New York, 1993; Vol. II.

(4) Klette, R.; Torring, J.; Plato, M.; MacMillan, F.; Rohrer, M.; Mobius, K. *J. Phys. Chem.* **1993**, *97*, 2015.

(5) Bratt, P. J.; Rohrer, M.; Krzystek, J.; Evans, M. C. W.; Brunel, L.-C.; Angerhofer, A. *J. Phys. Chem.* **1997**, *101*, 9686.

(6) Prisner, T. F.; McDermott, A. E.; Un, S.; Norris, J. R.; Thurnauer, M. C.; Griffin, R. G. *Proc. Natl. Acad. Sci. U.S.A.* **1993**, *90*, 9485.

(7) Prisner, T. F.; van der Est, A.; Bittl, R.; Lubitz, W.; Stehlik, D.; Möbius, K. *Chem. Phys.* **1995**, *194*, 361.

(8) Tang, J.; Bondeson, S.; Thurnauer, M. C. *Chem. Phys. Lett.* **1996**, *253*, 293.

(9) Kandrashkin, Y. E.; Salikhov, K. M.; Stehlik, D. *Appl. Magn. Reson.* **1997**, *12*, 141.

(10) Kirmaier, C.; Holten, D.; Debus, R.; Feher, G.; Okamura, M. Y. *Proc. Natl. Acad. Sci. U.S.A.* **1986**, *83*, 6407.

(11) Blankenship, R. E.; Parson, W. W. *Biochim. Biophys. Acta* **1979**, *545*, 429−444.

(12) Lui, B.; van Kan, P. J. M.; Hoff, A. J. *FEBS Lett.* **1991**, *289*, 23−28.

(13) Schelvis, J. P. M.; Liu, B.-L.; Aartsma, T. J.; Hoff, A. J. *Biochim. Biophys. Acta* **1992**, *1102*, 229−236.

(14) Utschig, L. M.; Greenfield, S. R.; Tang, J.; Laible, P. D.; Thurnauer, M. C. *Biochemistry* **1997**, *36*, 8548−8558.

(15) Hore, P. J.; In *Advanced EPR. Applications in Biology and Biochemistry*; Hoff, A., Ed.; Elsevier: Amsterdam, 1989.

(16) Closs, G. L.; Forbes, M. D. E.; Norris, J. R. *J. Phys. Chem.* **1987**, *91*, 3592.

(17) Thurnauer, M. C.; Norris, J. R. *Chem. Phys. Lett.* **1980**, *76*, 557.

(18) Füchsle, G.; Bittl, R.; van der Est, A.; Lubitz, W.; Stehlik, D. *Biochim. Biophys. Acta* **1993**, *142*, 23.

(19) Morris, A. L.; Norris, J. R.; Thurnauer, M. C. In *Reaction Centers of Photosynthetic Bacteria*; Michel-Beyerle, M.-E., Ed.; Springer-Verlag: Berlin, 1990.

(20) Morris, A. L.; Snyder, S. W.; Zhang, Y.; Tang, J.; Thurnauer, M. C.; Dutton, P. L.; Robertson, D. E.; Gunner, M. R. *J. Phys. Chem.* **1995**, *99*, 3854.

(21) Norris, J. R.; Morris, A. L.; Thurnauer, M. C.; Tang, J. *J. Chem. Phys.* **1990**, *92*, 4239.

(22) Hore, P. H. *Mol. Phys.* **1996**, *89*, 1195.

(23) Crespi, H. L. *Methods Enzymol.* **1982**, *88*, 3−5.

(24) Disselhorst, J. A. J. M.; van der Meer, H.; Poluektov, O. G.; Schmidt, J. *J. Magn. Reson.* **1995**, *A115*, 183.

(25) Chang, C.-H.; El-Kabbani, O.; Tiede, D.; Norris, J.; Schiffer, M. *Biochemistry* **1991**, *30*, 5352.

(26) Ermler, U.; Fritzsch, G.; Buchanan, S.; Michel, H. In *Research in Photosynthesis*; Murata, N., Ed.; Kluwer: Dordrecht, 1992; Vol. 1, p 341.

(27) Komiya, H.; Yeats, T. O.; Rees, D. C.; Allen, J. P.; Feher, G. *Proc. Natl. Acad. Sci. U.S.A.* **1988**, *85*, 9012.

(28) Klette, R.; Torring, J. T.; Plato, M.; Möbius, K.; Bönigk, B.; Lubitz, W. *J. Phys. Chem.* **1993**, *97*, 2015−2020.

(29) van der Est, A.; Bittl, R.; Abresch, E. C.; Lubitz, W.; Stehlik, D. *Chem. Phys. Lett.* **1993**, *212*, 561−568.

(30) Tang, J. *Chem. Phys. Lett.* **1998**, *290*, 49−57.

(31) Tang, J.; Thurnauer, M. C.; Norris, J. R. *Chem. Phys. Lett.* **1994**, *219*, 283−290.

(32) Kirmaier, C.; Holten, D.; Parson, W. W. *Biochim. Biophys. Acta* **1985**, *810*, 33−48.

(33) Marcus, R. A. *Annu. Rev. Phys. Chem.* **1964**, *15*, 155−196.

(34) Gunner, M. R.; Dutton, P. L. *J. Am. Chem. Soc.* **1989**, *111*, 3400.

(35) Budil, D. E. Ph.D. thesis, University of Chicago, Chicago, 1986.

(36) Volk, M.; Ogrodnik, A.; Michel-Beyerle, M. E. In *Anoxygenic Photosynthetic Bacteria*; Blankenship, R. E., Madigan, M. T., Bauer, C. E., Eds.; Kluwer: Dordrecht, 1995.

(37) Gilch, P.; Pollinger-Dammer, F.; Musewalk, C.; Michel-Beyerle, M. E.; Steiner, U. E. *Science* **1998**, *281*, 982.

(38) Chidsey, C. E. D.; Takiff, L.; Goldstein, R. A.; Boxer, S. G. *Proc. Natl. Acad. Sci. U.S.A.* **1985**, *82*, 6850.

(39) As a referee pointed out, one explanation might be a possible inhomogeneity of the samples and broad distributions of the k_Q rates. This could lead to different results for the optical experiment vs the EPR measurements, as different types of spectroscopy might be more sensitive to one or another end of the distribution of the k_Q or to the shape of the distribution. This suggestion has some merit. After submitting this manuscript for publication our preliminary transient optical measurements of the temperature dependence of k_Q in "slow" samples clearly show a multiexponential decay. This is a direct indication of a distribution of k_Q rates. On the other hand, we cannot make any quantitative analyses on the basis of experimental data at this point.

(40) Franzen, S.; Goldstein, R. F.; Boxer, S. G. *J. Phys. Chem.* **1990**, *94*, 5135−5149.

(41) van den Brink, J. S.; Hulsebosch, R. J.; Gast, P.; Hore, P. J.; Hoff, A. J. *Biochemistry* **1994**, *33*, 13668−13677.

(42) Tiede, D. M.; Vazquez, J.; Cordova, J.; Marone, P. A. *Biochemistry* **1996**, *35*, 10763−10775.